Design and Fabrication of Magnetically Functionalized Core/Shell Microspheres for Smart Drug Delivery

By *Xiuqing Gong, Suili Peng, Weijia Wen,* Ping Sheng,* and *Weihua Li*

The fabrication of magnetically functionalized core/shell microspheres by using the microfluidic flow-focusing (MFF) approach is reported. The shell of each microsphere is embedded with magnetic nanoparticles, thereby enabling the microspheres to deform under an applied magnetic field. By encapsulating a drug, for example, aspirin, inside the microspheres, the drug release of the microspheres is enhanced under the compression–extension oscillations that are induced by an AC magnetic field. This active pumping mode of drug release can be controlled by varying the frequency and magnitude of the applied magnetic field as well as the time profile of the magnetic field. UV absorption measurements of cumulative aspirin release are carried out to determine the influence of these factors. The drug release behavior is found to be significantly different depending on whether the applied field varies sinusoidally or in a step-function manner with time.

1. Introduction

Microcapsules or vesicles prepared by ''smart'' materials are receiving increasing attention owing to their capability of targeting a specific organ/tissue and triggering drug release through the application of an external stimulus.[1–4] These materials are stimuli-sensitive and can experience changes in either their structure or chemical characteristics, thereby offer the merits of a modulated drug release rate and a shortened tolerance time accompanying a constant drug release rate. Examples of smart materials that can be stimuli-sensitive include block copolymers,[5] polyelectrolyte multilayers,[6] and phospholipids.[7] The environmental triggering signals can arise from changes in temperature,[8] pH values,[9] electric field,[10] light,[11] or certain chemicals.[12] Another example of smart materials is magnetic material based composites. Extensive research efforts have been put into the development of magnetic drug carriers in clinical medicine. These carriers can interact with an external magnetic field positioned at a specified area targeted for drug delivery and magnetic resonance imaging.[13,14] Here we report the stimuli- sensitive shape change of magnetic particles as a new way in modulating drug release rate. We address the fabrication of core/shell microspheres that comprise magnetic shells encapsulating some water-soluble drug; these core/shell microspheres can respond to an AC magnetic field through oscillating shape variations that can in turn enhance the release of the encapsulated drug. The shell is composed of magnetite nanoparticles embedded in glutaraldehyde-crosslinked chitosan. This type of organic/inorganic magnetic shell shows interesting structural deformation under the application of a magnetic field. The compression–extension oscillations are controllable by varying the frequency, amplitude, and time profile of the alternating electric current applied to an electromagnet. As a consequence of such structural deformations, the drug release rate can be actively modulated. We carried out these experiments by using an aspirin solution as the encapsulated core of the microspheres to determine the drug release efficiency that can be realized.

To fabricate the core/shell microspheres, we use the microfluidic approach that has been popular for generating single- or multi-phase emulsions, for example, W/O/W (water/oil/water), O/O/W, and O/W/O emulsions.[15,16] The first step of the microfluidic approach is normally the formation of symmetric droplets in a two-phase or three-phase system by using either a T-junction geometry[17,18] or a microfluidic flow-focusing (MFF) device.[19,20] To obtain solidified particles, an interfacial chemical reaction or physical dewetting is induced to trap the droplets once they are formed. The interfacial solidifying methods include photopolymerization,[21–23] hydrolysis and condensation,[24] dewetting coacervation,[25] or other chemical reactions.[19,26] Here ''dewetting'' means drawing the solvent out of the droplet's outer layer so as to separate the inner and outer phases and to form a thin layer of polymersome. This approach exploits the molecular diffusion through a thin film

[*] Prof. W. Wen, P. Sheng
Department of Physics and
William Mong Institute of Nano Science and Technology
The Hong Kong University of Science and Technology
Clear Water Bay, Kowloon (Hong Kong)
E-mail: phwen@ust.hk
X. Gong, S. Peng
Nano Science and Technology Program
The Hong Kong University of Science and Technology
Clear Water Bay, Kowloon (Hong Kong)
Dr. W. Li
Faculty of Engineering
University of Wollongong
Wollongong NSW 2522 (Australia)

DOI: 10.1002/adfm.200801315

WILEY InterScience DISCOVER SOMETHING GREAT
© 2009 WILEY-VCH Verlag GmbH & Co. KGaA, Weinheim

either by evaporation[25] or by osmotic pressure.[19] In this work, we employed the MFF methodology to create a core/shell double emulsion, and then used the dewetting effect to dehydrate the outer layer of the emulsion. A crosslinking reaction helped to increase the mechanical strength of the core/shell structure.[27,28] The resultant magnetic core/shell microspheres were shown to exhibit magnetoelastic functionality.

2. Results and Discussion

To obtain the core/shell double emulsion, we first fabricated an MFF chip with polydimethylsiloxane (PDMS) by using soft lithography (Fig. 1).[29,30] It consists of a main flow channel with five inlets and a T-type side channel (labeled 4 in Fig. 1a). The channels are 200 μm in both depth and width. We used an aqueous solution of aspirin (1%, w/v) as the model drug to be infused through the middle channel (Fig. 1a, labeled 3). The aspirin solution injected was enveloped by streams composed of modified magnetite particles (2.5 g) in 150 mL of acetic acid (2% aqueous, w/v) and high molecular weight chitosan (1.5%, w/v) from two neighboring channels (Fig. 1a, labeled 2). The chemical hexadecane, with span-80 (0.5%, w/v), was used as the carrying fluid and injected through the outermost two channels (Fig. 1a, labeled 1). With proper control of the relative flow rates of the different streams, the innermost stream (aspirin solution) became unstable and broke into uniform droplets.[31] The core/shell double emulsion comprising an inner core of aspirin solution and an outer shell of high molecular weight chitosan, embedded with magnetic nanoparticles, was thus formed (Fig. 1e and Fig. 2a).

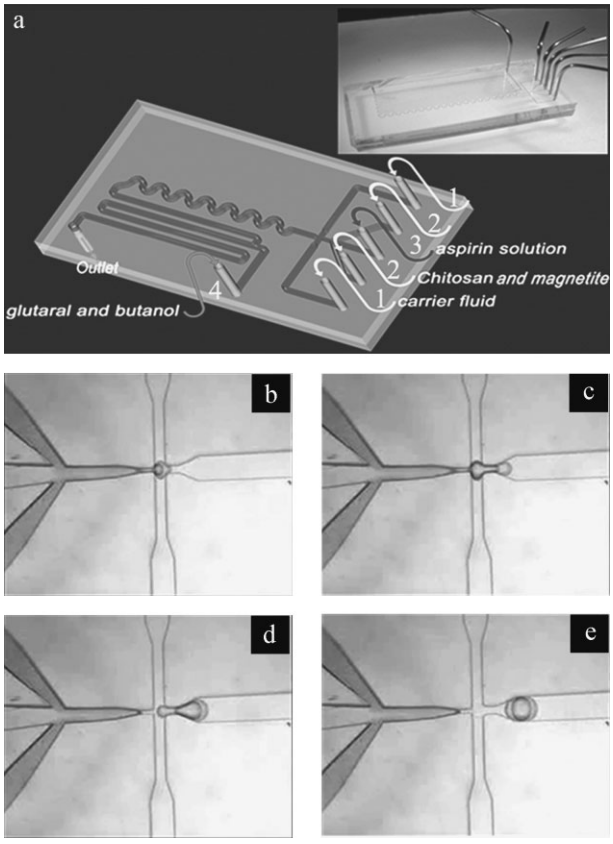

Figure 1. a) A schematic picture and a photograph (inset) of the MFF device; b–e) The formation process of the core/shell double emulsion. The width of the main channel shown in the figure is 200μm.

We employed the dewetting effect[25] and a crosslinking reaction to solidify the outmost layer/shell of the microspherical droplets. An additional channel (labeled 4 in Fig. 1a) was used to inject the dewetting solvent *n*-butanol and crosslinking reagent glutaraldehyde (10%, w/v, glutaraldehyde in butanol). The solubility of *n*-butanol in water is 9.1 mL/100 mL at room temperature. When the core/shell droplets (Fig. 2a) flowed through the mixture of glutaraldehyde and butanol, water in the droplets was gradually drawn out by butanol and, thus, a thin layer was visible (Fig. 2b and c). We also tried ethanol, 1-propanol (both are fully miscible in water), and 1-pentanol (3.3 mL/100 mL water) as the dewetting reagent. The time that the dewetting agent can fully dehydrate droplets varied (for ethanol and 1-propanol, the time was less than 5 s; for *n*-butanol and 1-pentanol, the required times were 20 and 60 s, respectively). In this experiment, the calculated residence time of droplets flowing in the channel is 5–10 s; thus, we used *n*-butanol to partially absorb the water. The produced particles were further baked at 60 °C for 2 h to facilitate the Schiff's base reaction between glutaraldehyde and chitosan (Fig. 2f). A crosslinked layer was eventually formed (Fig. 2d, e, and h). FTIR has confirmed the primary amide bands of chitosan at 1655 cm^{-1} split into peaks at 1635 and 1650 cm^{-1} (both are assigned to the C=N imine absorption[32,33]). The increased intensity of C–H stretching vibration frequency at 2936 cm^{-1} can also reflect the contribution of the glutaraldehyde molecules in the crosslinked chain (Fig. 2g).

If the residence time is much longer than the dehydrating time, over-permeation of water can occur, leading to the complete shrinkage of the core/shell microspheres (Fig. 2i). To prevent over-dehydration of the droplets, a quenching process was necessary to absorb butanol by adding a solution of oleic acid in hexane (30%, v/v). We used three syringe pumps to control the flow rates of the different liquids. The droplet sizes were adjustable in the range between 40 to 200 μm by varying the relative flow rates.

To confirm that we have fabricated the core/shell particles emulsion, we substituted the aspirin core with fluorescein isothiocyanate (FITC) solution. By detecting their fluorescence, we observed a fluorescent core and a nanoparticle-embedded shell (Fig. 3a). The particle has a soft shell of about 1 μm in thickness and a hollow core after freeze-drying (Fig. 3b and c). From the FTIR result, not all the chitosan has undergone the crosslinking reaction as evidenced by the free amines at 1560 cm^{-1}.[30] We suspect residual chitosan may exist in the interior of the microspheres as we can see a rough interior surface in the scanning electron microscopy (SEM) images. To confirm the existence of free chitosan, we mixed the particles with FITC solution. After stirring, we detected absorption at 495 nm, which is assigned to the maximum absorption wavenumber of FITC. This is based on the reaction between the isothiocyanate group of FITC and the primary amino group of chitosan.[34] The magnetic response of our core/shell microspheres is shown in Figure 3d.

© 2009 WILEY-VCH Verlag GmbH & Co. KGaA, Weinheim

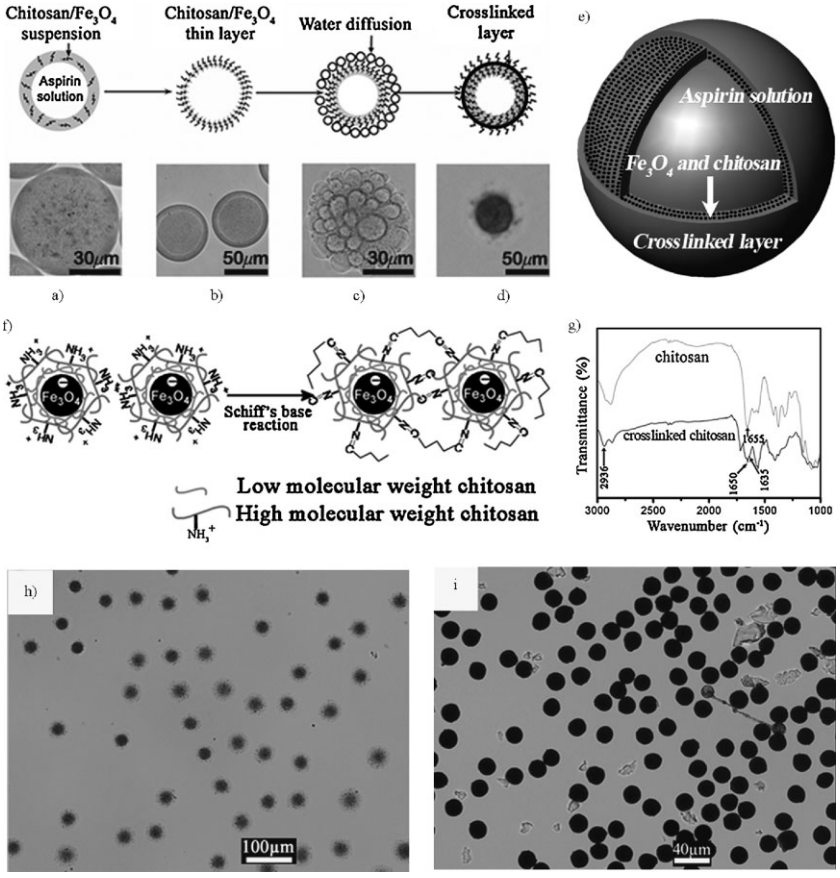

Figure 2. Structural evolution from double emulsion to core/shell particles: a) double emulsion, b) initial core/shell structure caused by the ''dewetting'' effect, c) dynamic permeation of water from inside the particle, d) a transparent outer layer formed through the crosslinking reaction. Cartoons in the top panel illustrate the process, and the pictures in the lower panel are the corresponding optical microscopy images of the droplets/particles. e) Schematic diagram indicating the structure of the microspheres. f) After the crosslinking reaction, the high molecular weight chitosan molecules are linked together by glutaraldehyde through a Schiff reaction. g) FTIR spectra between 3000 and 1000 cm^{-1}. h) Monodispersed particles corresponding to (d). i) Full shrinkage of particles leads to a brown color and reduced size.

Superparamagnetic behavior of the microspheres is evident from the measured results, where the saturation magnetization is approximately 12 emu g^{-1}.

It is interesting that the microspheres can change their shapes from spherical to spheroidal under an AC magnetic field. Figure 4 shows the elongation of the microspheres under 100, 200, and 300 G (1 G = 10^{-4} T) magnetic fields when the frequency is 5 Hz. The degree of extension can be adjusted by varying the strength of the magnetic field.[35] We counted 50 microspheres and plotted their aspect ratios as a function of the magnetic field. It was observed that when the microspheres changed their shapes from spherical to spheroidal, the aspirin solution was released through the crosslinked shell, detailed below.

To investigate the drug release efficiency through the microspheres' magnetically induced oscillatory deformations, magnetic fields of different strength, frequency, and time variation profile was applied to the sample. In the experiment, we used the dialysis technique[36] and the percentage of cumulatively released aspirin C can be defined as:

$$C = \frac{C_i}{C_a} \times 100 \quad (1)$$

Here C_i is a cumulative amount of released aspirin for each measurement, while C_a is the total amount of aspirin—the encapsulated amount. We define the total amount of aspirin as that in a 1 mL syringe which is 10 mg, as for each measurement 1 mL syringe of aspirin solution was used to make one dialysis bag. Each measurement was repeated three times and the average value was calculated.

The drug release characteristics of the core/shell microspheres under magnetic field are shown in Figure 5a and b, where it can be seen that when the frequency is fixed at 5 Hz, the applied magnetic field can enhance the drug release rate/efficiency as the strength varied from 0 to 300 G (Fig. 5a). Likewise, when the strength is fixed at 300 G, a higher frequency can increase the drug release rate/efficiency when the frequency was varied from 0 to 20 Hz (Fig. 5b). Hence, a stronger magnetic field at higher frequency implies a higher release rate. It can be seen from the insets in Figure 5a and b that, after 6 h, 9% of the enhanced drug release amount can be achieved by varying the strength. This should be compared with 26% by varying the frequency. Tables 1 and 2 list the amount of aspirin released under different magnetic fields and frequencies.

Figure 5c and d shows the effect of the time variation profile of the magnetic field on the drug release rate. Two types of voltage profiles, step function (inset of Fig. 5c) and sinusoidal (inset of Fig. 5d), were applied. In Figure 5c, it can be observed that both can result in a linear enhancement of drug-release percentage when the field strength was raised at a fixed frequency (20 Hz). But the step-function time profile shows a higher slope than the sinusoidal time profile. By fixing the magnetic field strength at 300 G, the two different time profiles yield almost the same aspirin release percentages for frequencies up to 5 Hz, as seen from Figure 5d, but beyond that the step-function time profile has a clear advantage in enhancing the aspirin release rate. From this experiment it is clear that the drug release rate is sensitive to sudden changes in the magnitude of the applied field, which is present in the step-function time profile but not in the sinusoidal profile.

3. Conclusion

We used the MFF approach to prepare core/shell microspheres encapsulated with an aqueous solution of aspirin. The resultant

WILEY InterScience® DISCOVER SOMETHING GREAT
© 2009 WILEY-VCH Verlag GmbH & Co. KGaA, Weinheim

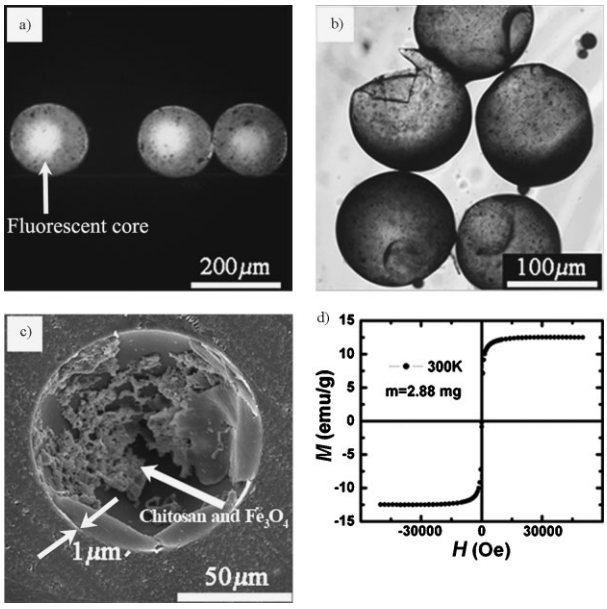

Figure 3. a) Core/shell double emulsion with a fluorescent core. b) Optical microscopy image of particles after freeze-drying. c) Scanning electron microscopy (SEM) image of the particle's cross section. Thickness of the thin layer labeled is about 1 μm. Unreacted chitosan and magnetite are located on the inner surface (indicated by the white arrow). d) Magnetization curve of the magnetic chitosan capsule.

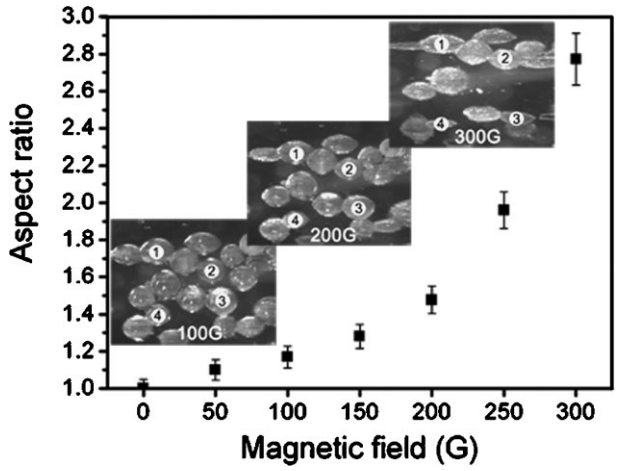

Figure 4. The aspect-ratio variation as a function of magnetic field obtained by analyzing 50 microspheres. The insets are the optical images of the microspheres when 100 G, 200 G, and 300 G field were applied. Elongation of the microspheres is visible as digits marking the reference points.

particles were demonstrated to be magnetically responsive. The aspirin release rate was measured by varying the strength of the applied magnetic field, its frequency, and its time profile. A particularly interesting conclusion is that a step-function time profile for the applied magnetic field is always more effective in enhancing the aspirin release rate.

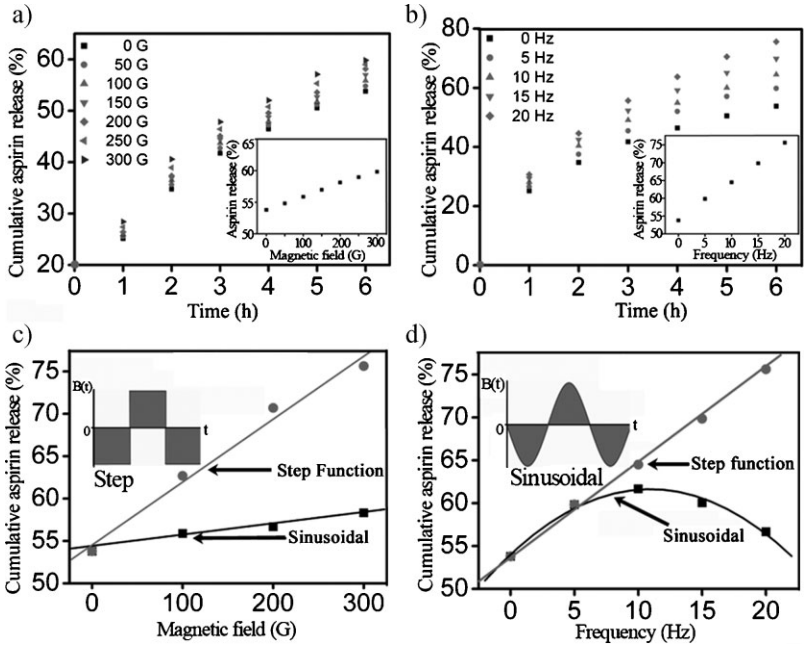

Figure 5. a) Cumulative aspirin release plotted as a function of time, for various applied magnetic field strengths. The frequency was fixed at 5 Hz. The inset shows the magnetic field dependence at 6 h. b) The same as (a), but the field strength was fixed at 300 G and the frequency was varied. The inset shows the frequency dependence at 6 h. c) Aspirin release percentage after 6 h, plotted as a function of magnetic field. The frequency was fixed at 20 Hz. One is for a step-function time variation of the magnetic field, the other is a sinusoidal time variation. The inserted picture shows a time profile of step function where the field is switched on and off. d) Aspirin release percentage after 6 h, plotted as a function of frequency. The field strength was kept at 300 G. The inset is a profile of the sinusoidal variation of the field.

4. Experimental

Materials: Low molecular weight chitosan, with a viscosity of 20 cps (1 cps = 10^{-3} Pa s) and a 75% degree of deacetylation, was employed to modify the magnetite particles; while high molecular weight chitosan, with a viscosity of 800 cps and a 75% degree of deacetylation, was infused to form the outer layer of the double emulsion. Hexadecane, with 0.5% (w/v) span-80 was used as the carrying fluid and a 1% (w/v) aqueous solution of aspirin was used as the test drug. 0.2% (w/v) FITC (+95% isomer, International Labrotary, USA) in a phosphate buffer solution (PBS) at pH 7.0 (Radiometer Copenhagen, Denmark) was used as a substitute to the aspirin solution. Butanol, used as the dewetting reagent, can allow the diffusion of water through droplets. A 70% aqueous solution of glutaraldehyde, which can react with chitosan, was employed as the crosslinking reagent [37, 38]. 30% (v/v) oleic acid in hexane was prepared to absorb butanol, with the purpose of quenching water diffusion induced by the dewetting effect. A silicon elastomer base and curing agent (Dow Corning Corporation, USA) were used to prepare the MFF chip. Cellulose membrane dialysis tubing, with a molecular weight cutoff of 12 000 Da (Sigma–Aldrich, USA), was used for the in vitro release study using the dialysis technique [36]. PBS, at pH 7.0, was chosen as the receiver solution to determine the aspirin amount diffused through the dialysis tubing. Milli-Q water (Millipore, USA) was used throughout the process.

Magnetic Nanoparticle Preparation: Magnetite nanoparticles were prepared by the coprecipitation method detailed by Massart [39]. Briefly, an aqueous solution containing 2 M hydrochloric acid and ferrous chloride was first mixed with 1 M ferrite chloride. 0.7 M ammonia solution

© 2009 WILEY-VCH Verlag GmbH & Co. KGaA, Weinheim

Table 1. The amount of aspirin [mg] released from the microspheres under different magnetic fields ($1\,G = 10^{-4}$ T) when the frequency is 5 Hz.

Time [h]	0 G	50 G	100 G	150 G	200 G	250 G	300 G
1	2.51	2.56	2.60	2.62	2.64	2.74	2.84
2	3.47	3.56	3.65	3.69	3.73	3.89	4.06
3	4.18	4.27	4.37	4.44	4.50	4.64	4.78
4	4.64	4.71	4.79	4.88	4.96	5.08	5.20
5	5.05	5.12	5.18	5.27	5.36	5.53	5.70
6	5.38	5.48	5.59	5.70	5.81	5.90	5.98

Table 2. The amount of aspirin [mg] released from the microspheres under different frequencies when the magnetic field is 300 G.

Time [h]	0 Hz	5 Hz	10 Hz	15 Hz	20 Hz
1	2.52	2.66	2.81	2.94	3.07
2	3.47	3.76	4.03	4.25	4.46
3	4.18	4.54	4.91	5.23	5.57
4	4.65	5.20	5.50	5.92	6.37
5	5.05	5.70	6.00	6.51	7.06
6	5.38	5.98	6.45	6.98	7.56

was then added. The mixture was stirred for 30 min and centrifuged at a speed of 10 000 rpm; the supernatant solution was removed by decantation. The precipitates were rinsed with deionized water until pH 7 was achieved and then freeze-dried. The magnetic nanoparticles were dispersed by an ultrasonic treatment for 3 h in an aqueous solution (100 mL) that comprised low molecular weight chitosan (1.5 g) and 2% (w/v) acetic acid. The suspension was subsequently centrifuged and freeze-dried to obtain the modified nanoparticles.

FITC-Labeled Microspheres: Freeze-dried microspheres (5 g) were added into methanol (25 mL) with FITC (25 mg); the mixture was stirred at room temperature for 24 h in the dark. After centrifugation, the sediment obtained was washed with methanol and water to remove the unreacted FITC. The obtained FITC-labeled particles were dissolved in 1% (w/v) acetic acid aqueous solution for measurement.

Characterization: The Fourier transform IR (FTIR) transmission spectrum was recorded on a Bio-Rad FTS6000 spectrometer with a DTGS detector. The number of scans was 32 with a spectral resolution of 4 cm^{-1}. The morphology of the microspheres was visualized with a JEOL-6700F scanning electron microscope with a target acceleration voltage of 5 kV. To prepare the SEM sample, we embedded microspheres (1 g) into a mixture (25:3 by volume) of epoxy resin and hardener (Struers A/S Company, Denmark). After solidification, we loaded it on a grinder–polisher (Buehler, USA) and polished it with a silicon carbide 800/2400 grit to observe the cross section. Microscopic analysis was carried out with a charge-coupled device (CCD) camera (DP70, Olympus) mounted on an inverted microscope (IX70, Olympus). Fluorescence observations were performed on a reflected fluorescence system equipped with a U-LH100HGAPO lamp housing and a IX2-RFACA motorized fluorescence mirror unit cassette (Olympus).

Measurements: Aspirin release characteristics were determined by UV-vis spectroscopy carried out using a Perkin–Elmer Lambda 20 UV/VIS spectroscope, where the aspirin concentration indication line was chosen at the maximum absorption wavelength of 296 nm. [40] For each measurement, microspheres (2 g) were stored in a dialysis bag (4 cm × 4 cm). The drug release efficiency was accessed in 3 mL PBS. In order to study the drug release activated under an applied magnetic field, an electromagnet with two parallel poles (Phewy Products, Germany) was used to generate a homogeneous magnetic field, in which the dialysis bag was placed. A function generator (PM 5139, Philips) and stereo power amplifier (216 THX, Lucasfilm Co.) were used to create pulsed signals. Absorption measurements were performed on an ND-1000 spectrophotometer at an excitation wavelength $\lambda_{ex} = 495$ nm (DIAMed).

Acknowledgements

Financial support of this work by Hong Kong RGC grant HKUST 621006 is hereby gratefully acknowledged.

Received: September 05, 2008
Published online: December 16, 2008

[1] Y. Ma, W. Dong, M. A. Hempenius, *Nat. Mater.* **2006**, *5*, 724.
[2] K. S. Soppimath, D. C. Tan, Y. Yang, *Adv. Mater.* **2005**, *17*, 318.
[3] F. Liu, A. Eisenberg, *J. Am. Chem. Soc.* **2003**, *125*, 15059.
[4] G. Ibarz, L. Dähne, E. Donath, H. Möhwald, *Adv. Mater.* **2001**, *13*, 1324.
[5] K. Kataoka, A. Harada, Y. Nagasaki, *Adv. Drug Delivery Rev.* **2001**, *47*, 113.
[6] G. B. Sukhorukov, A. A. Antipov, A. Voigt, E. Donath, H. Möhwald, *Macromol. Rapid Commun.* **2001**, *22*, 44.
[7] M. C. Sandström, L. M. Ickenstein, L. D. Mayer, K. Edwards, *J. Controlled Release* **2005**, *107*, 131.
[8] K. S. Soppimath, L. H. Liu, W. Y. Seow, S. Q. Liu, R. Powell, P. Chan, Y. Yang, *Adv. Funct. Mater.* **2007**, *17*, 355.
[9] Y. Sumida, A. Masuyama, M. Takasu, T. Kida, *Langmuir* **2001**, *17*, 609.
[10] I. C. Kwon, Y. H. Bae, S. W. Kim, *Nature* **1991**, *354*, 291.
[11] J. M. Park, S. Aoyama, W. Zhang, Y. Nakatsuji, I. Ikeda, *Chem. Commun.* **2000**, 231.
[12] K. Ishihara, N. Muramoto, I. Shinohara, *J. Appl. Polym. Sci.* **1984**, *29*, 211.
[13] I. Safarik, M. Safarýkova, *J. Chromatogr. B* **1999**, *722*, 33.
[14] P. Oswald, O. Clement, C. Chambon, E. Schouman-Claeys, G. Frija, *Magn. Reson. Imaging* **1997**, *15*, 1025.
[15] S. L. Anna, N. Bontoux, H. A. Stone, *Appl. Phys. Lett.* **2003**, *82*, 364.
[16] M. Seo, C. Paquet, Z. Nie, S. Xu, E. Kumacheva, *Soft Matter* **2007**, *3*, 986.
[17] T. Nisisako, T. Torii, T. Higuchi, *Lab Chip* **2002**, *2*, 24.
[18] P. Garstecki, M. J. Fuerstman, H. A. Stone, G. M. Whitesides, *Lab Chip* **2006**, *6*, 437.
[19] S. Takeuchi, P. Garstecki, D. B. Weibel, G. M. Whitesides, *Adv. Mater.* **2005**, *17*, 1067.
[20] P. Garstecki, H. A. Stone, G. M. Whitesides, *Phys. Rev. Lett.* **2005**, *94*, 164501.
[21] S. Xu, Z. Nie, M. Seo, P. Lewis, E. Kumacheva, H. A. Stone, P. Garstecki, D. B. Weibel, I. Gitlin, G. M. Whitesides, *Angew. Chem. Int. Ed.* **2005**, *44*, 724.
[22] H. Song, D. L. Chen, R. F. Ismagilov, *Angew. Chem. Int. Ed.* **2006**, *45*, 7336.
[23] M. Seo, Z. Nie, S. Xu, M. Mok, P. C. Lewis, R. Graham, E. Kumacheva, *Langmuir* **2005**, *21*, 11614.
[24] J. L. Steinbacher, R. W. Moy, K. E. Price, M. A. Cummings, *J. Am. Chem. Soc.* **2006**, *128*, 9442.
[25] R. C. Hayward, A. S. Utada, N. Dan, D. A. Weitz, *Langmuir* **2006**, *22*, 4457.
[26] S. L. Poe, M. A. Cummings, M. P. Haaf, D. T. Mcquade, *Angew. Chem. Int. Ed.* **2006**, *45*, 1544.
[27] M. Li, S. Cheng, H. Yan, *Green Chem.* **2007**, *9*, 894.
[28] M. M. Beppu, R. S. Viera, C. G. Aimoli, C. C. Santana, *J. Membr. Sci.* **2007**, *301*, 126.
[29] Y. Xia, G. M. Whitesides, *Annu. Rev. Mater. Sci.* **1998**, *28*, 153.
[30] X. Niu, M. Zhang, S. Peng, W. Wen, P. Sheng, *Biomicrofluidics* **2007**, *1*, 044101.
[31] T. Thorsen, R. Robert, F. Arnold, S. Quake, *Phys. Rev. Lett.* **2001**, *86*, 4163.
[32] J. D. Schiffman, C. L. Schauer, *Biomacromolecules* **2007**, *8*, 594.
[33] O. A. C. Monteiro, Jr, C. Airoldi, *Int. J. Biol. Macromol.* **1999**, *26*, 119.

WILEY InterScience® DISCOVER SOMETHING GREAT
© 2009 WILEY-VCH Verlag GmbH & Co. KGaA, Weinheim

[34] O. Hiraku, M. Yoshiharu, *Biomaterials* **1999**, *20*, 175.
[35] S. Peng, M. Zhang, X. Niu, W. Wen, P. Sheng, *Appl. Phys. Lett.* **2008**, *92*, 012108.
[36] E. Leo, R. Cameroni, F. Forni, *Int. J. Pharm.* **1999**, *180*, 23.
[37] S. R. Jameela, A. Jayakrishnan, *Biomaterials* **1995**, *16*, 769.
[38] S. R. Jameela, T. V. Kumar, A. V. Lal, A. Jayakrishnan, *J. Controlled Release* **1998**, *52*, 17.
[39] R. Massart, *IEEE Trans. Magn.* **1981**, *17*, 1247.
[40] S. Patnaik, A. K. Sharma, B. S. Garg, *Int. J. Pharm.* **2007**, *342*, 184.

© 2009 WILEY-VCH Verlag GmbH & Co. KGaA, Weinheim